

# Sensing of Fluctuating Nanoscale Magnetic Fields Using Nitrogen-Vacancy Centers in Diamond

L. T. Hall,<sup>1,\*</sup> J. H. Cole,<sup>1,2</sup> C. D. Hill,<sup>1</sup> and L. C. L. Hollenberg<sup>1</sup>

<sup>1</sup>Centre for Quantum Computer Technology, School of Physics, University of Melbourne, Victoria 3010, Australia

<sup>2</sup>Institute für Theoretische Festkörperphysik and DFG-Centre for Functional Nanostructures (CFN), Universität Karlsruhe, 76128 Karlsruhe, Germany

(Received 24 July 2009; published 25 November 2009)

New magnetometry techniques based on nitrogen-vacancy (NV) defects in diamond allow for the detection of static (dc) and oscillatory (ac) nanoscopic magnetic fields, yet are limited in their ability to detect fields arising from randomly fluctuating (FC) environments. We show here that FC fields restrict dc and ac sensitivities and that probing the NV dephasing rate in a FC environment should permit the characterization of FC fields inaccessible to dc and ac techniques. FC sensitivities are shown to be comparable to those of ac magnetometry and require no additional experimental overhead or sample control.

DOI: 10.1103/PhysRevLett.103.220802

PACS numbers: 07.55.Ge, 07.79.-v, 81.05.Uw

The exploitation of controlled quantum systems as ultrasensitive nanoscale detectors has tremendous potential to advance our understanding of complex processes occurring in biological and condensed-matter systems at molecular and atomic scales [1–3]. The stringent requirements for high sensitivity and spatial resolution has led to suggestions of using spin-based quantum systems as nanoscale magnetometers [4] or of imaging through detection of sample induced decoherence [5]. One particularly attractive physical platform to implement these ideas is the nitrogen-vacancy (NV) center in diamond [Fig. 1(a)], chosen for its long coherence times at room temperature and convenient optical readout of the spin state [6] [Fig. 1(b)]. The robust properties of NV nanodiamonds make them ideal for biological applications [7,8]. As such, NV centers have been the focus of recent proposals to image static (dc) and oscillating (ac) magnetic fields [9,10], which have since been demonstrated experimentally [11–13]. However, many important biological and condensed-matter systems exhibit nonsinusoidal fluctuating magnetic fields with extremely low or zero mean values [Fig. 1(d)]. An important question is therefore to what extent these quantum based magnetometry techniques are applicable to such situations. In this Letter, we address this by quantifying the detection sensitivities for these modes for samples with fluctuations characterized by the rms field and dominant spectral frequency. The results indicate that by probing the dephasing rate of a spin qubit placed in such environments, one can characterize the underlying fluctuation rates and rms field strengths that would be otherwise inaccessible with the use of dc and ac magnetometry techniques, thereby opening the way for noninvasive nanoscale imaging of a range of biological and condensed-matter systems.

The theory behind the detection of magnetic fields using quantum systems is heavily reliant on the phase estimation program of quantum metrology, particularly the determination of coupling parameters that are constant in time. In

the context of dc magnetometry, this corresponds to measurement of the first moment (the mean) of the magnetic field strength. For zero mean fields, complex microwave control pulse sequences are necessary. For fields exhibiting oscillatory (ac) time dependence with which either a spin-echo or Carr-Purcell-Meiboom-Gill [14] sequence may be synchronized, sensitivities are predicted to be as low as  $3 \text{ nT Hz}^{-1/2}$  [10], based on the standard quantum limit.

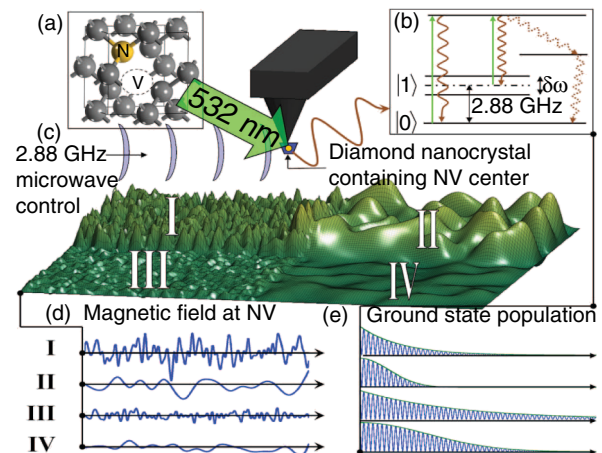


FIG. 1 (color online). Schematic of a scanning NV qubit magnetometer-decoherence probe for the detection of nanoscale field fluctuations. (a) NV center diamond lattice defect. (b) NV spin detection through optical excitation and emission cycle. (c) Microwave control of the NV spin state and 532 nm optical pulse for readout. (d) Simulated magnetic field signals at the NV probe corresponding to regions I–IV of an inhomogeneous test sample with different fluctuation amplitudes and frequency spectra. (e) The corresponding NV ground state populations show that the regions can be distinguished by the dephasing information. I: Strong, rapid fluctuations  $\rightarrow$  fast exponential dephasing. II: Strong, slow fluctuations  $\rightarrow$  fast Gaussian dephasing. III: Weak, rapid fluctuations  $\rightarrow$  slow exponential dephasing. IV: Weak, slow fluctuations  $\rightarrow$  slow Gaussian dephasing.

Excellent agreement between theory and experiment has been demonstrated in [12]. Such techniques require accurate knowledge of the field dynamics which may not be available or, more commonly, the field may exhibit a stochastic time dependence. Examples include nuclear dipole fields of ion channels [15] [Fig. 2(a)] and lipid bilayers in biological cell membranes [16], Overhauser fields in Ga-As quantum dots [17], and even self-diffusing water molecules [18,19] [Fig. 2(b)]. In what follows, we investigate the effects of a more general fluctuating (FC) field on the dephasing of a spin qubit as the primary detection mechanism and the implications for the characterization of the magnetic field from the surrounding environment. In this sense, we are estimating the second moment of the field strength and the corresponding temporal dynamics.

A spin qubit placed in a randomly fluctuating magnetic environment will experience a complex sequence of phase kicks, leading to an eventual dephasing of the population spectrum. For a NV center, this will be in addition to the intrinsic sources of dephasing, which are due to paramagnetic impurities in the diamond lattice [20]. The dephasing rate can be quantified via repeated projective measurements of the qubit state, and the corresponding dephasing envelope,  $\mathcal{D}(\tau)$ , can be determined via a suitably chosen quantum state reconstruction technique. We use the technique of Hamiltonian characterization [21] rather than quantum tomography techniques, as it requires only a single measurement basis yet is robust in the presence of dephasing [22].

The motivation for the environment model used here comes from consideration of magnetic dipoles in motion. Other models in which a two level system is coupled to a bath of bistable fluctuators have been previously considered [23–26]. These models, however, do not capture the dephasing effects due to gradual transitions between environmental states in slowly fluctuating fields. Later we will show this to be of particular importance in the case of spin-echo based experiments. Additionally, these models require a large number of fluctuators to model a continuous signal. In contrast, we wish to consider the dephasing effects of small numbers of spins in motion.

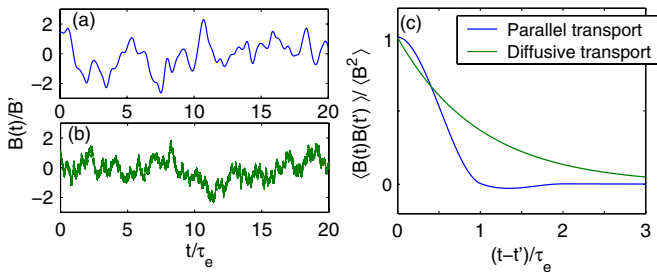


FIG. 2 (color online). Simulated magnetic field traces,  $B(t)/B'$ , for (a) a channel of dipoles in unidirectional motion and (b) a self-diffusing dipole bath. (c) Temporal correlation function  $\langle B(t)B(t') \rangle / \langle B^2 \rangle$ . Time axes are rescaled by  $\tau_e$ .

Consider a qubit with gyromagnetic ratio  $\gamma_p$  undergoing a  $\frac{\pi}{2} - \tau - \frac{\pi}{2}$  Ramsey sequence in the presence of a classical FC magnetic field,  $B(t)$ . An example of such a field due to a unidirectional spin current is shown in Fig. 2(a) and that of a bath of self-diffusing spins in Fig. 2(b). The field has mean  $\langle B \rangle \equiv B_0$ , standard deviation  $\sqrt{\langle B^2 \rangle - \langle B \rangle^2} \equiv B'$ , and typical fluctuation rate  $f_e \equiv 1/\tau_e$ , where  $\tau_e$  is the self-correlation time of the field [Fig. 2(c)]. This gives rise to two natural frequency scales, given by  $\omega_0 = \gamma_p B_0$  and  $\omega' = \gamma_p B'$ . The average precession frequency of the qubit is set by  $\omega_0$  and is decoupled from all dephasing effects for cases where  $\omega', f_e \ll \omega_0$ . Additional relaxation processes may dominate the qubit evolution when this condition is violated; however, such cases are not considered here since we are interested in the characterization of weak magnetic fields. The nature of the dephasing will depend on the fluctuation rate of the environment,  $f_e$ , or more specifically the magnitude of the quantity defined by  $\Theta \equiv f_e/\omega'$ . In the case of  $\Theta \gg 1$ , or fast-fluctuation limit (FFL), the qubit will experience many environmental fluctuations during its natural time scale. Whilst  $B'$  need not necessarily be normally distributed, the accumulated phase error of the qubit at some time  $t \gg 1/f_e$  will be, by way of the central limit theorem. As such, the variance of the phase error at time  $t \gg 1/\omega'$  will be  $\langle \Delta \phi^2 \rangle \sim t \gamma_p^2 B'^2 / f_e$ , giving rise to a FFL dephasing rate of

$$\Gamma_{\text{fast}}(B', f_e) = \frac{\gamma_p^2 B'^2}{2f_e}. \quad (1)$$

This is akin to the motional narrowing result from NMR and reproduces the ubiquitous exponential dephasing envelope given by  $\mathcal{D}_{\text{fast}}(t) = \exp(-\Gamma_{\text{fast}} t)$ .

In the slow-fluctuation limit (SFL), where  $\Theta \ll 1$ , we note that the magnetic field may be locally approximated by a Taylor expansion in  $t$  about some initial time  $t_0$ :  $B(t) = \sum_{k=0}^N \frac{1}{k!} \frac{d^k B}{dt^k} \Big|_{t_0} (t - t_0)^k \equiv \sum_{k=0}^N a_k (t - t_0)^k$ , where each of the  $a_k$  has a specific statistical distribution containing information about the  $k$ th order derivative of  $B(t)$  and thus gives rise to a different dephasing channel.

For the special case where the  $a_k$  are normally distributed with mean  $\mu_k$  and variance  $\sigma_k^2$  (as consistent with random dipole motion), the resulting density matrix following the free-evolution time  $\tau$  but prior to the second  $\pi/2$  pulse is defined by  $\rho_{11} = \rho_{22} = 1/2$  and  $\rho_{12} = \rho_{21}^* = \prod_{k=0}^{\infty} \mathcal{D}_{\text{slow}}^{(k)}(\tau) \Omega_{\text{slow}}^{(k)}(\tau)$ , where

$$\mathcal{D}_{\text{slow}}^{(k)}(t) = \exp[-(\Gamma_{\text{slow}}^{(k)} t)^{2k+2}], \quad (2)$$

and

$$\Omega_{\text{slow}}^{(k)}(t) = \exp[-i(\omega_{\text{slow}}^{(k)} t)^{k+1}]. \quad (3)$$

Thus, we see the emergence of a hierarchy of dephasing and beating channels, with the dephasing rates and beat frequencies of the  $k$ th channel given by

$$\Gamma_{\text{slow}}^{(k)} = \left( \frac{1}{\sqrt{2}} \frac{\sigma_k \gamma_p}{k+1} \right)^{1/(k+1)} \quad (4)$$

and  $\omega_{\text{slow}}^{(k)} = (\frac{\mu_k \gamma_p}{k+1})^{1/(k+1)}$ , respectively. In the case of the zeroth order channel, this corresponds to the rigid lattice result from NMR, and we have  $\sigma_0^2 = \langle B^2 \rangle - \langle B \rangle^2$ . This effect will be suppressed by a spin-echo pulse sequence. For the first order channel, we may approximate  $\sigma_1^2 \sim (\langle B^2 \rangle - \langle B \rangle^2) f_e^2$ .

The relative contributions of each channel to the overall dephasing rate of the qubit depend explicitly on the dynamics of the field; however, dominance of the zeroth order channel (i.e.,  $\Gamma_{\text{slow}}^{(0)} > \Gamma_{\text{slow}}^{(j)}, \forall j \geq 1$ ) is a necessary and sufficient condition for the system to exist in the slow-fluctuation regime,  $\Theta \ll 1$ . This justifies the use of the Taylor expansion since the resulting polynomial may be well approximated by a low-order truncation.

The intermediate regime of  $\Theta \sim 1$  is more complicated. Figure 3(a) shows dephasing envelopes for various values of  $\Theta$ . For times much longer than  $\tau_e$ , pure exponential dephasing behavior is observed in all cases (with a dephasing rate  $\Gamma_{\text{fast}}$ ); however, fast fluctuating environments still exhibit slow (Gaussian) dephasing behavior on time scales  $\tau$  where  $\omega' \tau < \sqrt{2}/\Theta$ . If  $\Theta$  is large, contributions to  $\mathcal{D}$  from the  $\Gamma_{\text{slow}}^{(k)}$  will decay rapidly. The abrupt transition from  $\mathcal{D}_{\text{slow}} \rightarrow \mathcal{D}_{\text{fast}}$  is shown more clearly in the corresponding inset.

Before proceeding to the specific NV implementation, we summarize the different field detection protocols. While dc detection involves letting the qubit evolve under the influence of a constant or near static background field, ac detection requires driving the sample at a particular frequency  $\nu$  while timing the spin-echo pulse synchronously. In both cases, the qubit phase shift, proportional to the time integral of the magnetic field, is detected. For FC fields, the accumulated phase is instead random, and

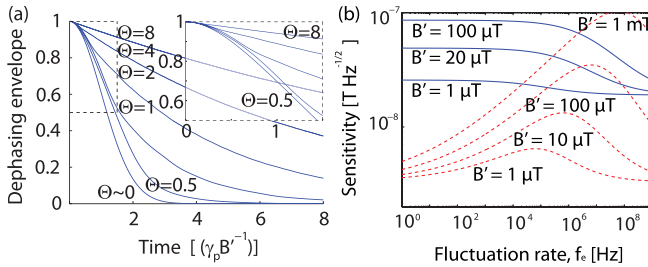


FIG. 3 (color online). (a) Plot of simulated dephasing envelopes for  $N_s = 10^4$  runs, showing agreement with Eqs. (1) and (2). Time is in units of  $(\gamma_p B')^{-1}$ . (inset) Zoomed plot showing that fast fluctuating environments still exhibit nonexponential dephasing for short time scales  $\tau$ :  $\omega' \tau < \sqrt{2}/\Theta$ . (b) dc [solid (blue) line] and ac [dashed (red) line] magnetic field sensitivities as a function of  $f_e$  for different contours of  $B'$ . The largest effect on  $\eta_{\text{ac}}$  comes from FC regimes in which  $\Theta \sim 1$ , away from which  $\eta_{\text{ac}} \rightarrow \frac{\pi \exp(\tau/T_2)^3}{2\gamma_p C \sqrt{\tau}} = 3 \text{ nT Hz}^{-1/2}$ . Assumed parameter values are  $T_2^* = 1 \mu\text{s}$ ,  $T_2 = 300 \mu\text{s}$ , and  $C = 0.3$ .

detection is achieved via a change in the qubit decoherence rate [5], which can be obtained from a spin-echo measurement in a similar manner to the ac case, albeit with no synchronization required.

For the purpose of comparison with existing spin-based magnetometer proposals, we take the NV center as our example qubit. The Hamiltonian used to describe the time evolution of a NV- center is given by  $\mathcal{H} = \mathbf{S} \cdot \mathbf{D} \cdot \mathbf{S} + \hbar \gamma_p \mathbf{B} \cdot \mathbf{S} + \mathcal{H}_{\text{other}}$ , where  $\mathcal{H}_{\text{other}}$  describes higher order effects such as hyper-fine splittings, etc., which can be ignored in the present context. We consider weak external fields such that  $|\gamma_p B'| \ll D$ , thereby ensuring the crystal-field splitting tensor,  $\mathbf{D}$ , sets the quantization axis of the NV centre and that  $\omega' \ll \omega_0$ .

The shot-noise-limited dc sensitivity for a NV-based magnetometer subject to a Ramsey-style pulse sequence is given by [10]  $\eta_{\text{dc}} \equiv B_{\text{min}} \sqrt{T} \approx (\gamma_p C \sqrt{\tau})^{-1}$ , where  $\sqrt{T}$  and  $C$  represent the combined effects of spin projection and photon shot noise for  $N_s$  measurements ( $C \rightarrow 1$  for the ideal case),  $\tau$  is the free-evolution time of the qubit, and  $T = N_s \tau$  is the total averaging time. Dephasing times due to nearby paramagnetic lattice impurities will in general be different for different centers and will thus require individual characterization. For comparison with [10], we take  $\tau = T_2^* \sim 1 \mu\text{s}$ . We emphasize that the expression for  $\eta_{\text{dc}}$  applies solely to the imaging of dc magnetic fields where the dephasing of the qubit is exclusively due to intrinsic crystal effects. If the sample produces a fluctuating field of sufficient amplitude, the dephasing time ( $1/\Gamma$ ) may be shorter than  $T_2^*$ , resulting in poorer static field sensitivity. In this context,  $\eta_{\text{dc}}$  refers to the sensitivity with which the mean field,  $\langle B \rangle$ , may be measured as the field fluctuates over the course of the experiment. To gain insight into the effect of FC fields on the dc field sensitivity, we consider again a  $\frac{\pi}{2} - \tau - \frac{\pi}{2}$  sequence. The dc sensitivity as a function of  $B'$  and  $f_e$  is shown in Fig. 3(b). From this, we see that fluctuating environments can have a dramatic effect on

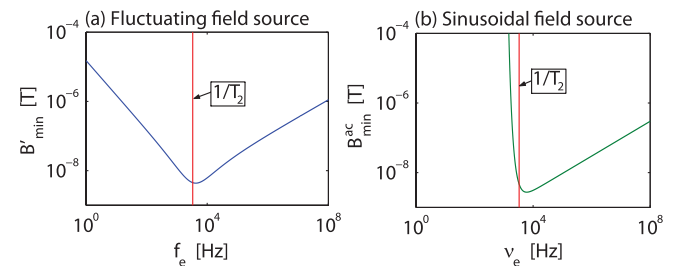


FIG. 4 (color online). (a) Minimum resolvable FC field strength,  $B_{\text{min}}$ , versus environmental fluctuation rate,  $f_e$ , for  $T = 1 \text{ s}$  averaging time. In contrast to the ac case, a FC detection requires no prior knowledge of fluctuation time scales. (b) Minimum resolvable ac field amplitude,  $B_{\text{min}}^{\text{ac}}$ , versus field oscillation frequency,  $\nu_e$ , for  $T = 1 \text{ s}$  averaging time in the absence of environmental noise ( $B' = 0$ ). Here we have assumed that the ac field is initialized in phase with the probe qubit and that the  $\pi$  pulse of a spin-echo sequence coincides with the first zero crossing of the field.

the dc field sensitivity of a NV-based magnetometer, depending on both field strength and fluctuation frequency.

Using coherent control techniques (spin echo [27], for example), we may extend the dephasing time of the NV center to  $T_2 \sim 300 \mu\text{s}$ , as dictated by the 1.1% carbon-13 content in the lattice. The case of perfectly oscillatory magnetic fields, in which the  $\pi$  pulse coincides with the first zero crossing of the magnetic field, has been considered in detail in [10], giving ac sensitivities as low as  $\eta_{\text{ac}} \approx \frac{\pi \exp(\tau/T_2)^3}{2\gamma_p C \sqrt{\tau}} \approx 3 \text{ nT Hz}^{-1/2}$  [Fig. 4(b)]. As with dc magnetometry, the ac sensitivity will be strongly dependent on the FC characteristics of the environment, as shown in Fig. 3(b) as a function of  $B'$  and  $f_e$ .

We now study the magnetometer's sensitivity to a more general class of fluctuating fields via consideration of the induced dephasing rate. For a  $\frac{\pi}{2} - \frac{\tau}{2} - \pi - \frac{\tau}{2} - \frac{\pi}{2}$  pulse sequence, the probe will show decreased sensitivity to environments for which  $f_e < 1/\tau$ . For  $\Theta \gg 1$ , the effect will be negligible. For  $\Theta \ll 1$ , this may appear problematic; however, complete insensitivity only comes with  $f_e \rightarrow 0$ . A spin-echo sequence will modify the  $\mathcal{D}_{\text{slow}}^{(k)}$  via  $\Gamma_{\text{slow}}^{(k)} \mapsto (1-2^{-k})^{[1/(k+1)]} \Gamma_{\text{slow}}^{(k)}$ ; thus, only the effects of the zeroth order dephasing channel will vanish. Perturbations on the dephasing rate may be measured from  $(1 - \mathcal{D})_{\text{min}} = \frac{\exp[(\tau/T_2)^3]}{C \sqrt{N_s}}$  [10,20]. This implies an optimal free-evolution time of  $\tau \sim T_2/\sqrt[3]{6}$ . Thus we find that perturbations on the  $1/T_2$  dephasing rate as slow as 200 Hz for exponential dephasing and 800 Hz for Gaussian dephasing may be detected by this method after 1 s of averaging time. By performing measurements of the total dephasing rate,  $\Gamma$ , both the field variance and the average fluctuation rate may be inferred from Eqs. (1) and (4). Of course, the question remains of which fluctuation regime in which a given sample system resides. In the absence of any prior knowledge of the environment being measured, this question may be answered via determination of the shape of the dephasing envelope, a task to which the Hamiltonian characterization method is well suited [5].

The optimal FC sensitivity will occur when  $\Theta \sim 1$ , since this ensures maximal dephasing for a given field variance. Considering the special case of pure exponential decay, we therefore expect an optimal sensitivity of  $\eta_{\text{fc}} = \frac{e^{1/6}}{C \gamma_p \sqrt{T_2}} = 1.7 \text{ nT Hz}^{-1/2}$ . However, such sensitivity may be difficult to realize due to memory effects in the fluctuating environment. For systems that satisfy  $\Theta \gg 1$ , thus exhibiting long-time exponential dephasing behavior, Gaussian dephasing is still exhibited for  $\tau < 1/f_e$  [Fig. 3(a)]. For spin-echo experiments, the effect is worsened as the dominant contribution to  $\mathcal{D}_{\text{slow}}$  comes from  $k = 1$ . Taking this into consideration, the minimum resolvable field obtained after  $T = 1$  s averaging time is plotted in Fig. 4(a) against  $f_e$ . We see that FC field strengths as low as 4.5 nT may be achievable after  $T = 1$  s averaging time ( $N_s \sim 3000$ ) and that the qubit will be sensitive to FC fields fluctuating on

time scales much slower than  $1/T_2$ . This is in direct contrast with the ac case, which shows poor sensitivity to fields oscillating with periods less than  $T_2$  [Fig. 4(b)].

We have theoretically investigated the effects of a fluctuating magnetic field on a NV center spin qubit. This analysis was used to place new limits on the sensitivity with which the mean field strength may be measured. Furthermore, we have built upon the idea of decoherence microscopy [5] to theoretically demonstrate the ability of a NV center to measure field strengths and fluctuation rates of randomly fluctuating magnetic fields. This analysis shows that the methods presented here require no experimental resources beyond those of existing techniques, no prior control or knowledge of the external field, and thus may be implemented with current technology.

We gratefully acknowledge discussions with A. Greentree, M. Testolin, F. Jelezko, and J. Wrachtrup. This work was supported by the Australian Research Council (ARC) and the Alexander von Humboldt Foundation.

\*lthall@physics.unimelb.edu.au

- [1] K. Hasselbach, C. Veauvy, and D. Mailly, *Physica (Amsterdam)* **332C**, 140 (2000).
- [2] J. R. Kirtley *et al.*, *Appl. Phys. Lett.* **66**, 1138 (1995).
- [3] R. C. Black *et al.*, *Appl. Phys. Lett.* **62**, 2128 (1993).
- [4] B. M. Chernobrod and G. P. Berman, *J. Appl. Phys.* **97**, 014903 (2005).
- [5] J. H. Cole and L. C. L. Hollenberg, *Nanotechnology* **20**, 495401 (2009).
- [6] F. Jelezko and J. Wrachtrup, *Phys. Status Solidi B* **203**, 3207 (2006).
- [7] F. Neugart *et al.*, *Nano Lett.* **7**, 3588 (2007).
- [8] C. C. Fu *et al.*, *Proc. Natl. Acad. Sci. U.S.A.* **104**, 727 (2007).
- [9] C. L. Degen, *Appl. Phys. Lett.* **92**, 243111 (2008).
- [10] J. M. Taylor *et al.*, *Nature Phys.* **4**, 810 (2008).
- [11] G. Balasubramanian *et al.*, *Nature (London)* **455**, 648 (2008).
- [12] J. R. Maze *et al.*, *Nature (London)* **455**, 644 (2008).
- [13] G. Balasubramanian *et al.*, *Nature Mater.* **8**, 383 (2009).
- [14] S. Meiboom and D. Gill, *Rev. Sci. Instrum.* **29**, 688 (1958).
- [15] B. Hille, *Ionic Channels of Excitable Membranes* (Sinauer Associates, Sunderland, 2001), 3rd ed.
- [16] M. Patra *et al.*, *Biophys. J.* **84**, 3636 (2003).
- [17] D. J. Reilly *et al.*, *Phys. Rev. Lett.* **101**, 236803 (2008).
- [18] V. I. Tikhonov and A. A. Volkov, *Science* **296**, 2363 (2002).
- [19] A. Rahman and F. H. Stillinger, *J. Chem. Phys.* **55**, 3336 (1971).
- [20] L. Childress *et al.*, *Science* **314**, 281 (2006).
- [21] J. H. Cole *et al.*, *Phys. Rev. A* **71**, 062312 (2005).
- [22] J. H. Cole *et al.*, *Phys. Rev. A* **73**, 062333 (2006).
- [23] A. Shnirman *et al.*, *Phys. Rev. Lett.* **94**, 127002 (2005).
- [24] J. Schrieffer *et al.*, *New J. Phys.* **8**, 1 (2006).
- [25] E. Paladino *et al.*, *Phys. Rev. Lett.* **88**, 228304 (2002).
- [26] Y. M. Galperin *et al.*, *Phys. Rev. Lett.* **96**, 097009 (2006).
- [27] F. Jelezko *et al.*, *Phys. Rev. Lett.* **92**, 076401 (2004).